3rd Workshop on CFD Uncertainty Analysis
October 23-24, 2008, Lisbon, Portugal

Application of Error Scaling Method in Conjunction with GCI

F. Elizalde-Blancas, E. Karaismail, I. B. Celik
Mechanical and Aerospace Engineering Department
West Virginia University
Morgantown WV, 26506 (USA)

ABSTRACT

The assessment of numerical uncertainty in CFD (Computational Fluid Dynamics) relies on the estimation of the true discretization error which is defined as the difference between the exact (commonly unknown) solution to the partial differential equation and the numerical solution obtained from a discretized equation on a certain grid. To determine the extrapolated exact solution to zero-grid cell size, Richardson extrapolation method is commonly used but this method has limited success and requires calculations on at least three and sometimes up to 5 or 6 grids. Even then questions related to non-monotonic convergence or divergence, the anomalies concerning the observed (or apparent) order of the computations can not be resolved. The technique proposed in this study attempts to avoid much of the difficulties of Richardson extrapolation and is based on the refinement of ideas presented by Celik and Li [1] concerning the relation between the approximate error and the true error. The proposed method is verified using manufactured solutions for a steady state, incompressible, 2-D turbulent flow emulating a boundary layer type flow. Then, it is applied to the case of flow over a backward facing space (Ercoftac Classic Database C-30). With the help of a manufactured solution provided in [2], the true error and other relevant uncertainty measures are analyzed. In the backward facing step case experimental results published by Driver and Lee [3] are compared with numerical solutions along with the calculated numerical uncertainties. The numerical simulations were performed using the commercial flow solver FLUENT along with some user defined functions.

1.0 INTRODUCTION

Along with the rapid increase in applications of CFD the interest in formulating some kind of quality control on the CFD solutions has increased. The uncertainty measures are usually based on some error estimates. The errors are primarily related to iteration convergence, grid convergence, and modeling errors among many others. This paper focuses on grid-convergence error also referred to as discretization errors. The iteration errors can be significant [4-7] however, in this work we reduce them to very small values so that they do not pollute the solution, hence the dominant numerical error is associated with discretization. The recommended method for discretization error estimation is the Richardson extrapolation (RE) method [8, 9]. This method has been studied by many researchers and its shortcomings have been widely investigated [10-19]. But, the RE method is far from perfect. The local RE values of the predicted variables may not exhibit a smooth, monotonic dependence on grid resolution, and in time dependent calculations, this non-smooth response becomes a function of time and space. Nonetheless, it is currently the most robust method available for the prediction of numerical

uncertainty. The method presented here can be considered as a variant of RE with more desirable features. Since there are many ways for estimating numerical uncertainty and errors, which are based on certain assumptions, such as monotonic convergence and being in the asymptotic range in case of RE, it is imperative that these methods be also validated using some benchmarks.

In this study the performance of the Approximate Error Scaling (AES) method when used in conjunction with the Grid Convergence Index (GCI) uncertainty estimation method is evaluated in assessing the numerical uncertainty. Then the same methodology is then applied to the case of flow over a backward facing step. Even though the flow regime in the boundary layer type flow (MS) is turbulent; the numerical solutions are carried out for pseudo-laminar flow taking advantage of the known exact solution. This was done in order to avoid the errors implicit in turbulence models. The transformation from turbulent to laminar flow was done by defining a momentum source term which precludes the pressure gradient term; for more details see [20]. In the backward facing step (BFS) case two turbulence models were used; Spalart-Allmaras model and standard k-ε model. In both of the test cases (MS and BFS) commercial flow solver FLUENT 6.3 is used for numerical simulations with various grid densities. Also these numerical simulations were performed using 1st and 2nd order upwind discretization schemes for the convective terms. User Defined Functions (UDFs) were used to prescribe boundary conditions specified in the problem and the sources in the case of the MS.

2.0 ERROR ESTIMATION METHOD

The method developed to predict the true error is a variant of the extrapolation method proposed by Celik *et al*. [1, 21, 22] named Approximate Error Scaling method (AES). This method assumes that the true error, E_t is proportional to the approximate error, E_a, (see Appendix for more details) that is

$$E_t^h = cE_a^h \tag{1}$$

where c represents the global proportionality constant.
The true error is defined by

$$E_t^h = \phi - \phi_h \tag{2}$$

and the approximate error given by

$$E_a^h = \phi_h - \phi_{\alpha h} \tag{3}$$

In Eqn. 3, α is the grid refinement or coarsening factor i.e. $\alpha_1=h_2/h_1$, $\alpha_2=h_3/h_2$, etc., where h_i represents the average grid size, also $h_1<h_2<h_3$ which means that subscript "1" denotes the smallest grid size (finest grid) and subscript "3" the coarsest grid.

In order to apply Eq. (1) three grid calculations (triplet) are needed. The post-processing of the numerical solutions on three different grids (ϕ_1, ϕ_2, ϕ_3) and the use of Eq. (1) enable determination of the local proportionality constant $c_{i,j}$ given by

$$c_{i,j}^1 = \frac{\phi_2^{i,j} - \phi_1^{i,j}}{\phi_3^{i,j} - 2\phi_2^{i,j} + \phi_1^{i,j}} \tag{4}$$

$$c_{i,j}^2 = \frac{\phi_3^{i,j} - \phi_2^{i,j}}{\phi_3^{i,j} - 2\phi_2^{i,j} + \phi_1^{i,j}} \tag{5}$$

The global proportionality constant c is calculated from the local constants as follows

$$c = \frac{1}{2} \frac{\| c_{i,j}^1 \|_\infty + \| c_{i,j}^2 \|_\infty}{N} \tag{6}$$

and the operator

$$\| c_{i,j} \|_\infty = \sum_{k=1}^{N} \left| c_{i,j} \right| \tag{7}$$

N in Eqs. (6) and (7) represents the total number of cells in the coarse grid. It is important to note that ϕ in Eqs. (4) and (5) represents each of the variables solved by the numerical calculations i.e. x-velocity component, y-velocity component and pressure when solving the Navier-Stokes equations for laminar flow in 2-D, therefore there is a global proportionality constant for each variable being solved.

3.0 UNCERTAINTY ESTIMATION METHOD

Once the global proportionality constant has been calculated as shown by Eq. (6) and making use of the relationship between the true error and the approximate error as given by Eq. (1) the uncertainty can be calculated using the GCI uncertainty estimator. The calculation of the uncertainty is based on the use of the fine and medium grids from the same triplet used to calculate the global proportionality constant. Re-writing Eq. (1) for the grids mentioned above

$$E_t^{fm} = cE_a^{fm} \tag{8}$$

where the superscript *fm* means that interpolation was performed from the fine grid to the medium grid. The definitions of the true and approximate errors shown in Eq. (8) are given by

$$E_t^{fm} = \phi_{ext}^{fm} - \phi_{fm}^{num} \tag{9}$$

$$E_a^{fm} = \phi_{fm}^{num} - \phi_m^{num} \tag{10}$$

where ϕ_{ext}^{fm} represents the extrapolated value at zero grid size which is an estimate of the analytical value. Substituting Eqs. (9) and (10) in Eq. (8) and solving for ϕ_{ext}^{fm} we get

$$\phi_{ext}^{fm} = \phi_{fm}^{num} + c\left(\phi_{fm}^{num} - \phi_m^{num}\right) \tag{11}$$

Then the uncertainty is calculated using the GCI which is given by

$$GCI = 1.25 \left| \frac{\phi_{ext}^{fm} - \tilde{\phi}_f}{\tilde{\phi}_f} \right| \tag{12}$$

where $\tilde{\phi}_f$ is the interpolated value from the numerical solution on the fine grid.

The methodology described previously for the calculation of the proportionality constant as well as for the uncertainty is the same when applied to local quantities or integral quantities.

4.0 MATHEMATICAL FORMULATION AND NUMERICAL SETTINGS

In this work, two test cases are studied. The first test case emulates the boundary layer type flow which has a manufactured solution that satisfies identically the continuity and the momentum equations in the turbulent regime for an incompressible flow over a stationary wall. For more detailed information see [2, 20]. The second test case corresponds to flow over a backward facing step (Ercoftac Classic Database C-30) in the turbulent regime. In both cases CFD calculations were performed using the commercial software FLUENT 6.3.

4.1 Case of Boundary Layer Type Flow (Manufactured Solution)

In the case of the MS the actual flow regime corresponds to a turbulent flow since the Reynolds number is 10^6. However, as the principal objective of this work is to assess the numerical uncertainty, the error induced by the turbulence model was eliminated by modifying the equations in such a way that the Navier-Stokes equations are solved for laminar flow and the turbulence effects of the flow were introduced as source terms in the momentum equations, see [20].

The computational domain for the MS is defined on a square with $0.5 \leq x \leq 1$ and $0 \leq y \leq 0.5$. Except for the south (bottom) boundary, the boundary conditions prescribed were the analytical velocity profiles expressed in terms of x and y components. This was accomplished by making use of UDFs. The south boundary was set as a wall with the no-slip condition.

In order to assess the numerical uncertainty several cases were run. The cases considered differ from each other in their grid density. Two sets of cases were defined as shown in Table 1. An orderly grid refinement was done between each case for every set. In each set the average grid size was decreased by circa a factor of four (i.e. grid doubling in both directions)

Table 1 Grid sets for the cases studied for uncertainty assessment (MS)

Case	Set I	Set II
1	10x10	15x15
2	19x19	30x30
3	40x40	60x60
4	80x80	120x120

The selected grids were structured, non-uniform with an expansion ratio of 0.95 in y-direction. The grid in y-direction is finer near the south boundary in order to predict, with reasonable accuracy, the velocity gradients inside the wall boundary layer. Along the x-direction the grid is uniform. All the cases shown in Table 1 were run with 1st and 2nd order upwinding schemes for the convective terms.

4.2 Case of Flow Over a Backward Facing Step

As mentioned previously the flow regime for the BFS case is turbulent with a Reynolds number of 5×10^4 and a reference velocity of 44.2 m/s. Here the Reynolds Averaged Navier-Stokes (RANS) equations are solved along with the one equation Spalart-Allmaras turbulence model and with the two equations standard k-ε turbulence model.

In a similar way as in the manufactured solution case, use of UDFs to prescribe the boundary conditions was needed in the flow problem over the backward facing step. At the inlet of the backward facing step, profiles of x-velocity component and modified turbulent viscosity were

prescribed when the Spalart-Allmaras turbulence model was used. Profiles of turbulent kinetic energy and turbulent dissipation rate at the inlet of the backward facing step were also prescribed when the standard k-ε model was used. These inlet profiles were provided by the organizers of the 2006 Lisbon Workshop [2] as Fortran functions. At the outlet, pressure was prescribed as constant. The rest of the boundaries were treated as smooth walls (no roughness) with the no slip condition. Along with the standard k-ε model the approach of standard wall functions was used as the near-wall treatment. The computational domain is $-4H \leq X \leq 40H$ and $0 \leq Y \leq 9H$, where H is the height of the step (1.27 cm) and also the reference length. The origin of the coordinate system is located at the lower corner of the step and the height of the inlet section is 8H.

The grids used for the BFS consisted of 20774 (143x150) cells for the finest grid (G1), 344 (18x20) cells for the coarsest grid (G4). The medium grids have approximately 5146 (72x74) cells (G2) and 1312 (36x38) cells (G3). The refinement factor between consecutive grids was 2 in both directions. The four grids were structured, uniform in x-direction and non-uniform in y-direction. The expansion ratio was not constant, varying in the range from 0.7 to 1.0 from coarsest to finest grid in different sub-regions. The grid is finer near the walls and in the shear layer region. As in the case of MS the four grids described above for the BFS case were run with 1st and 2nd order upwinding schemes for the convective terms. Converged solution for G1 using the standard k-ε model and 2nd order discretization could not be achieved.

5.0 RESULTS

All the data presented in this work was obtained with 1st and 2nd order upwinding schemes (for convection) in the commercial flow solver FLUENT. The scheme applied to diffusion terms is second order central differencing. Double precision was used for all the calculations so that the round-off errors are minimized and thus can be considered negligible. The solution was considered a converged solution when scaled residuals were reduced to machine accuracy. The highest scaled residual for the MS case was in the order of 10^{-15} and for the BFS in the order of 10^{-9} for the second order scheme using the Spalart-Allmaras model and in the order of 10^{-15} with the standard k-ε model in both 1st and 2nd order schemes.

5.1 Case of Boundary Layer Type Flow (Manufactured Solution)

The convergence of the flow variables (u, v and P) in the case of the MS using the pseudo-laminar model for 1st and 2nd order calculations were analyzed in three points of interest for all the grids listed in Table 1. These three points are (0.6, 0.001), (0.75, 0.002) and (0.9, 0.2) and from now on they are called first, second and third point respectively. In Fig. 1 the grid convergence at the first and third points is shown for the relevant flow variables.

From Fig. 1 it can be seen that away from the wall (third point) 1st and 2nd order calculations show monotonic convergence while close to the wall only pressure shows a monotonic convergence. Close to the wall (first point) both velocity components seem to converge non-monotonically when the governing equations are discretized with first order approximations. In general, 2nd order calculations show better monotonic convergence than 1st order calculations. Also very near the wall (first point) u velocity is far from convergence.

The analytical values of the flow variables at the same three points mentioned above are presented in Table 2. Comparing the information shown in Table 2 with the numerical solutions obtained in the finest grid at the same points (Fig. 1), it can be concluded that numerical calculations converge to the analytical solution in 1st and 2nd order calculations for the y-velocity

component and pressure in the three points. The u velocity converges to the MS value in all points only with 2nd order calculations and, with 1st order it converges only away from the wall.

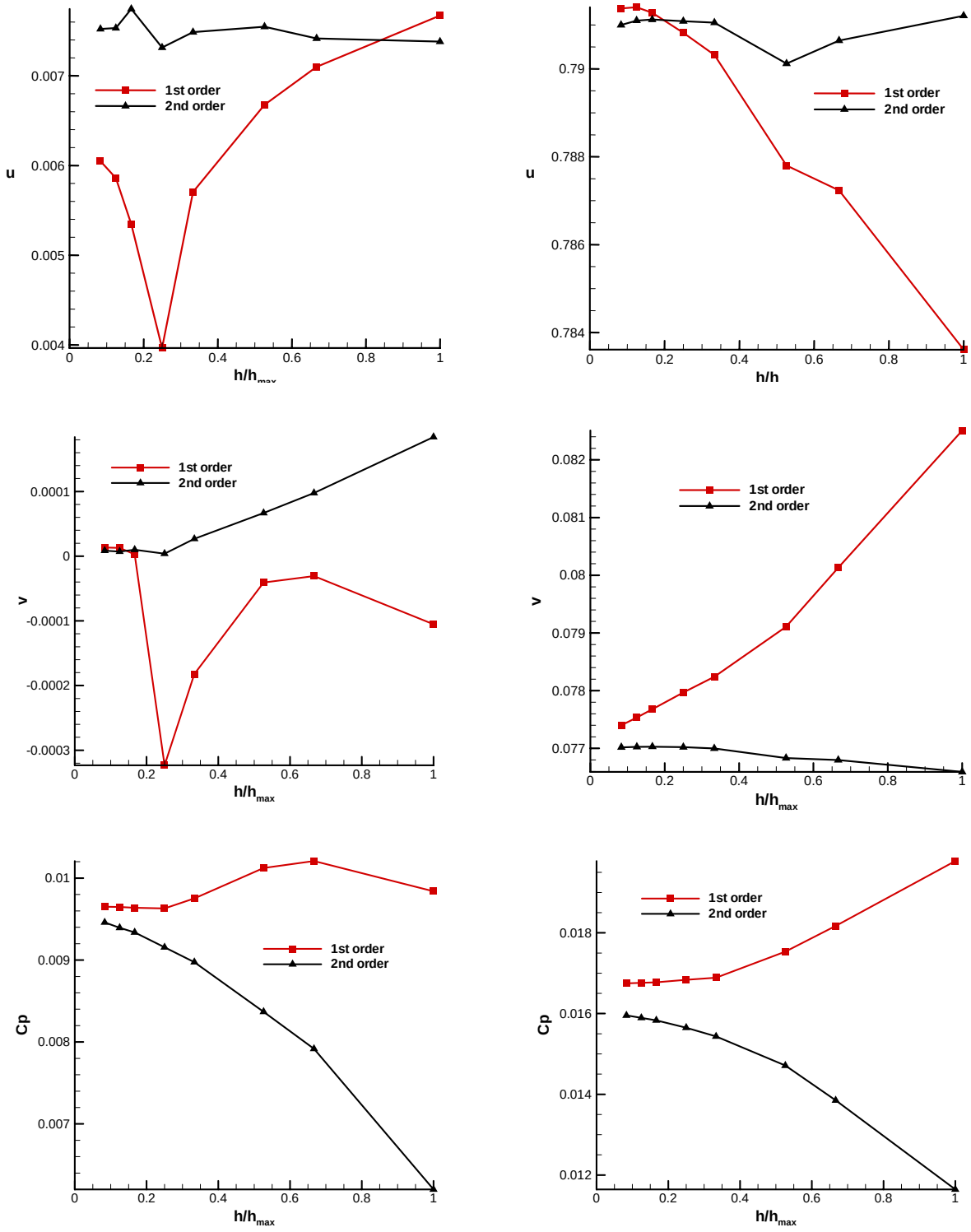

(a) **(b)**

Figure 1 Convergence of flow variables at points (a) x=0.6, y=0.001 and (b) x=0.9, y=0.2

Table 2 Exact values of the flow variables

Point	u	v	P
(0.6, 0.001)	7.5224e-3	6.2686e-6	0.0096148
(0.75, 0.002)	0.012035	1.6046e-5	0.019173
(0.9, 0.2)	0.791275	0.077041	0.016148

From now on, uncertainties in the same three points of interest are reported. For brevity only the results obtained with the coarse triplet from set I (see Table 1) are presented, but all the other triplet combinations from the two sets of grids are briefly discussed. In case of MS, true uncertainties U_t are calculated and compared with the estimated uncertainties to assess the performance of the uncertainty estimation method proposed in this work. This can be considered, in a way, validation of the proposed error estimation method. In Table 3 the estimated and true uncertainties for the flow variables are presented for the 1st order calculations. The same information is shown in Table 4 but with results obtained from 2nd order calculations.

Table 3 Calculated values and uncertainties from 1st order calculations based on the coarse triplet from set I

Position	X=0.60, Y=0.001	X=0.75, Y=0.002	X=0.90, Y=0.200
u*	3.966e-3	-1.167e-3	0.790818
U(u) %	125.55	1222.5	0.2387
U_t(u) %	112.11	1413.7	0.072
v*	-3.2332e-4	-2.55e-3	0.07797
U(v) %	243.33	188.82	2.827
U_t(v) %	127.42	125.78	1.486
P*	9.631e-3	0.019424	0.016837
U(P) %	9.908	3.562	8.143
U_t(P) %	0.205	1.614	5.108

* the reported values for u,v and P are those interpolated from the solution on the grid 40x40

As can be seen from 1st order calculations (Table 3) the estimated uncertainty bounds the true uncertainty except for the second point in the x-velocity component. In Table 4 (2nd order calculations) the true uncertainty is bounded by the estimated uncertainty at all the points and for all flow variables. When using the fine triplet from the same set of grids (set I) two and six cases are not bounded for 1st and 2nd order calculations, respectively. This apparently indicates that the proposed uncertainty estimation method performs better when a coarse triplet i.e. coarse grids, is used. When using the grid set II, which is a set with finer grids compared to set I, it was observed that the performance of the method decreased. In summary, when using grid set I, and considering first and second order calculations, the estimated uncertainty bounds 94% and 55% of the cases using the coarse and fine triplet, respectively. With set II, 72% of the cases were bounded with the coarse triplet and only 33% with the fine triplet. It is important to note that the estimated uncertainties; either bounded or unbounded, in general, are very close to the true uncertainties, therefore the 33% of the bounded cases reported above can be misleading about the performance of the method.

It is important to note that these uncertainty calculations were performed with solutions that do not necessarily converge monotonically and/or to the analytical solution.

Table 4 Calculated values and uncertainties from 2nd order calculations based on the coarse triplet from set I

Position	X=0.60, Y=0.001	X=0.75, Y=0.002	X=0.90, Y=0.200
u*	7.314e-3	0.012071	0.791084
U(u) %	4.46	9.26	0.36
U_t(u) %	3.55	0.37	0.03
v*	3.9515e-6	2.3611e-5	0.077021
U(v) %	1220.52	132.73	0.12
U_t(v) %	73.30	40.05	0.03
P*	0.009155	0.018703	0.015650
U(P) %	10.14	26.31	7.05
U_t(P) %	6.27	3.14	3.98

* the reported values for u,v and P are those interpolated from the solution on the grid 40x40

The proportionality constants calculated with Eq. (6) are presented in Table 5. It is interesting that the proportionality constants do not converge to the theoretical value (asymptotic range) i.e. 1.33 for 2nd order and 2.0 for 1st order calculations, when the grid is refined using set I, but they approach the theoretical values with set II. In general, the proportionality constants for 2nd order calculations are smaller than those calculated from first order calculations, which is expected since 2nd order calculations are usually more accurate solutions.

Table 5 Global proportionality constants for coarse triplet from set I

Order	**u**	**v**	**P**
1st	1.999	1.311	1.455
2nd	0.9718	0.9702	0.9850

The integral quantity called friction resistance was calculated along with its uncertainty at the bottom wall. These results are reported in Table 6 using the coarse grid triplet of set I along with 1st and 2nd order calculations. Also in the same table, the calculated proportionality constant is reported. Again, it can be seen that the proportionality constant for 2nd order calculations is smaller than that for the 1st order.

Table 6 Calculated values and uncertainties for the friction resistance at the bottom wall based on the coarse triplet from set I

Order	**C_F**	**U(C_F) %**	**C**
1st	1.155024e-6	418.1	3.819
2nd	3.189875e-6	3.43	1.672

In general it can be concluded that uncertainties calculated from 2nd order calculations are smaller than those obtained from 1st order calculations as it is expected.

5.2 Case of Flow Over a Backward Facing Step

Similarly to the MS case, three points of interest were selected in the BFS case, these points are located at (0, 1.1H), (H, 0.1H) and (4H, 0.1H), where H is the step height. The convergence of the flow variables using both turbulence models and 1st and 2nd order discretizations were analyzed at these points. The convergence at all these points shows in most of the solved variables to be non-monotonic. As an example of convergence, Fig. 2 shows the convergence of the two velocity components and pressure at point (0, 1.1H) with both turbulence models and with first and second order calculations. In the reattachment point and in integral quantities such as friction resistance and pressure resistance the convergence showed a monotonic trend in some cases. When the Spalart-Allmaras model was used monotonic convergence in the reattachment point and in friction resistance was observed with 1st and 2nd order calculations. The standard k-ε model showed monotonic convergence in 1st order calculations.

In Table 7 the calculated values for x and y-velocity components as well as pressure and turbulent viscosity along with their estimated uncertainties are reported for the three points of interest mentioned above. This information was obtained with both turbulence models, using 2nd order discretization schemes and the coarse triplet for the BFS case. From Table 7 it can be seen that the estimated uncertainties using the Spalart-Allmaras model are smaller than those estimated with the standard k-ε model. Completely opposite to the behavior observed in local quantities, when integral quantities such as friction and pressure resistance are analyzed, they show that uncertainties estimated with the standard k-ε model are smaller as shown in Table 8. Also in Table 8 the calculated proportionality constant used by the uncertainty estimation method here proposed is reported. A trend similar to that shown by local flow variables is observed by the reattachment point as shown in Table 9.

Different to the MS case, in the BFS case there is no exact solution to compare and assess the performance of the uncertainty estimation method, however there is experimental data available [3] which can be used for these purposes. In Fig. 3 experimental and numerical x and y-velocity profiles at x=H are shown. The numerical profiles from 2nd order calculations obtained with both turbulence models used in this work are presented along with their calculated validation uncertainties in this figure. The numerical results correspond to the solution on the finer grid of the coarse triplet. As can be seen from Fig. 3 the predicted velocity along with its validation uncertainty of the standard k-ε model binds more experimental data than the Spalart-Allmaras turbulence model and this is because (i) the standard k-ε model predicts better velocity fields and (ii) as mentioned above the uncertainties calculated for the standard k-ε model are larger than those estimated for the Spalart-Allmaras model. Similar trends are observed at other two different x-locations.

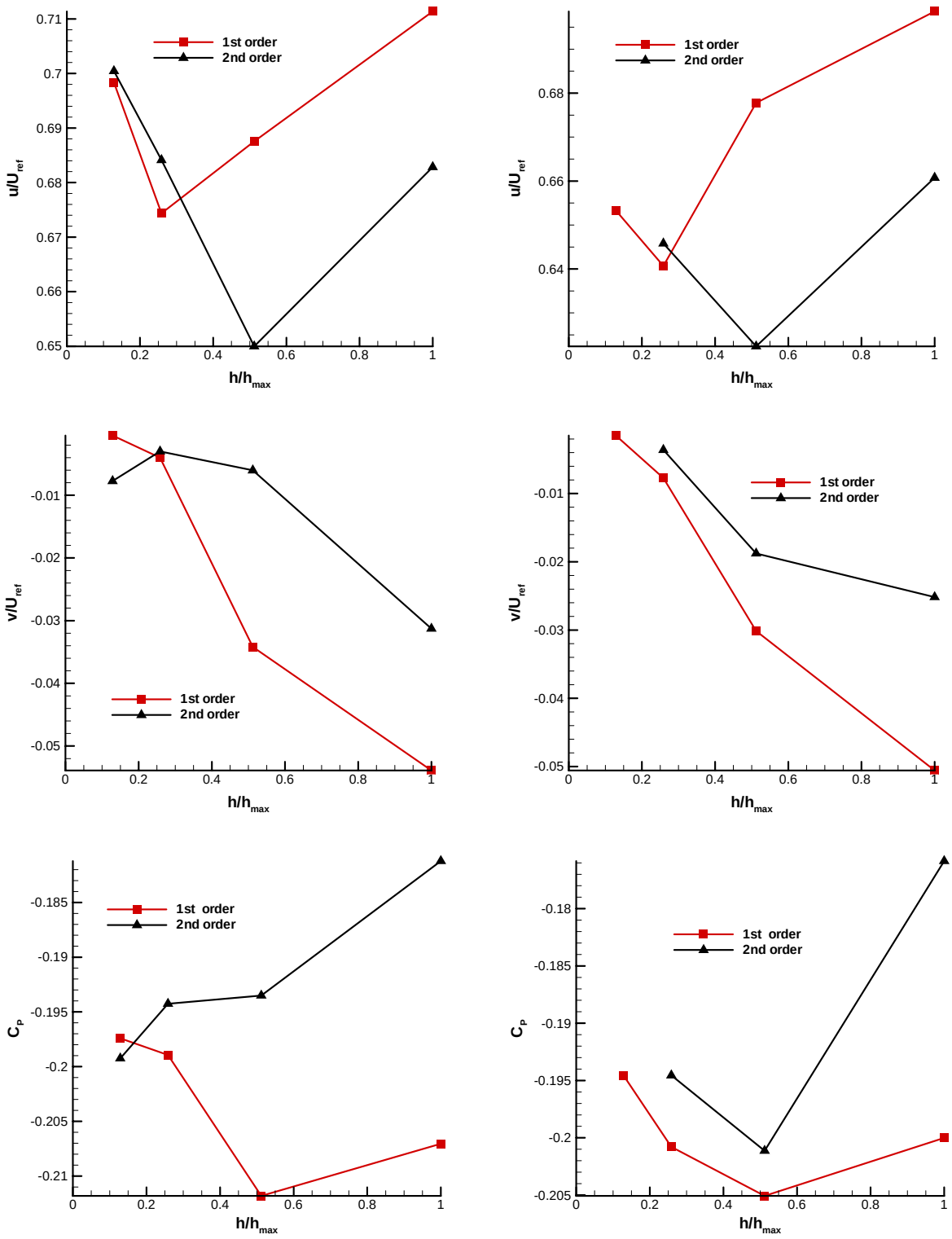

Figure 2 Convergence of flow variables at points x=0, y=1.1H using (a) Spalart-Allmaras model and (b) standard *k*-ε model

Table 7 Calculated values and uncertainties for flow variables from 2nd order calculations based on the coarse triplet using Spalart-Allmaras and standard *k*-ε turbulence model

S&A			
Position	x=0.0, y=1.1H	x=H, y=0.1H	x=4H, y=0.1H
u*	0.684136	-0.196959	-0.113545
U(u) %	5.41	27	54
v*	-0.003005	0.012537	-0.011620
U(v) %	73.36	42.46	7.46
P*	-0.1942	-0.2375	-0.0930
U(P) %	3.11	1.9	11.28
ν_t	8.8191e-4	7.4879e-4	1.2413e-3
U(ν_t) %	38.11	6.08	3.28
Standard *k*-ε			
Position	x=0.0, y=1.1H	x=H, y=0.1H	x=4H, y=0.1H
u*	0.645811	-0.095006	-0.071516
U(u) %	7.85	82.35	309.48
v*	-0.003602	0.008161	-0.005873
U(v) %	249.6	16.46	82.36
P*	-0.1945	-0.2165	-0.1259
U(P) %	4.31	4.94	61.61
ν_t	2.3575e-4	2.3687e-3	5.6166e-3
U(ν_t) %	1269.82	413.88	120.76

* the reported values are those calculated from the solution on the finest grid of the triplet

Table 8 Calculated values and uncertainties for the friction resistance at bottom and top walls and pressure resistance from 2nd order calculations based on the coarse triplet using Spalart-Allmaras and standard *k*-ε turbulence model

Turbulence model	**$C_{F,b}$**	**U($C_{F,b}$) %**	**C**
Spalart-Allmaras	0.023812	30.46	5
Standard *k*-ε	0.0318969	3.183	0.50
	$C_{F,t}$	**U($C_{F,t}$) %**	**C**
Spalart-Allmaras	0.044202	1.906	1.236
Standard *k*-ε	0.043287	24.485 %	5.0
	C_P	**U(C_P) %**	**C**
Spalart-Allmaras	0.105674	3.31	0.5
Standard *k*-ε	0.106512	9.69 %	0.5

Table 9 Calculated values and uncertainties for the reattachment point from 2nd order calculations based on the coarse triplet

Turbulence model	**x_{reatt}/H**	**U(x_{reatt}/H) %**	**C**
Spalart-Allmaras	5.771560	2.9	0.7123
Standard *k*-ε	5.548599	24.36	0.5

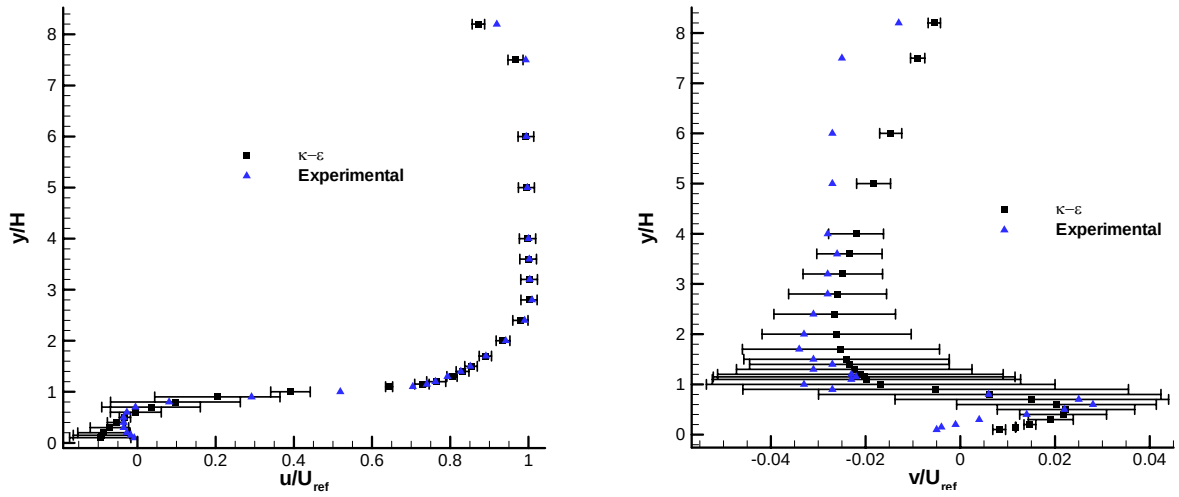

(a) **(b)**

Figure 3 Velocity profiles and their uncertainties at x=H from 2nd order calculations with the standard *k*-ε model on the coarse triplet

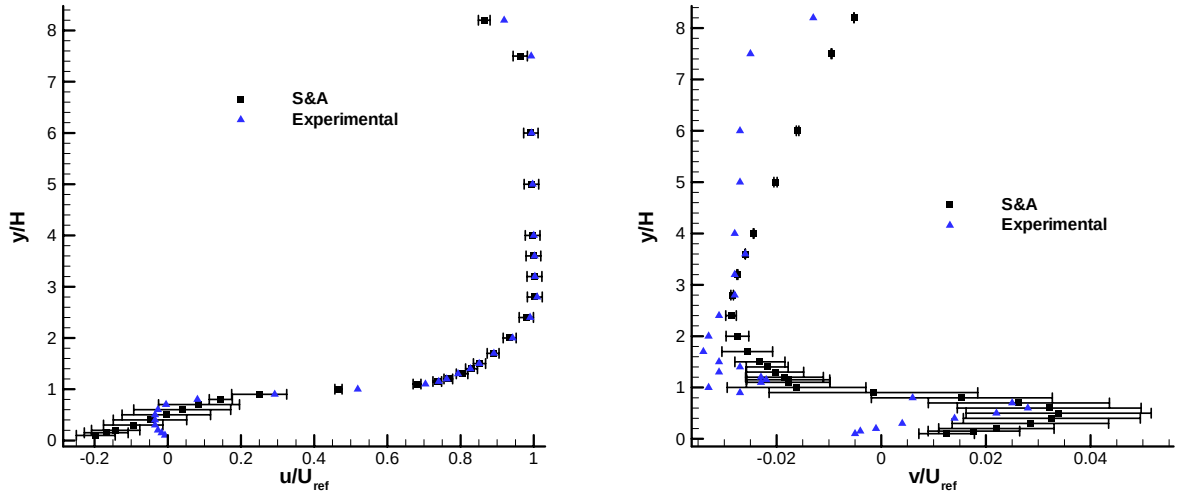

(a) **(b)**

Figure 4 Velocity profiles and their uncertainties at x=H from 2nd order calculations with the Spalart-Allmaras model on the coarse triplet

6.0 CONCLUSIONS

Numerical calculations were performed using first and second order discretization schemes in two test cases; (i) in a boundary layer-type flow which has a manufactured solution and (ii) in a flow over a backward facing step. The uncertainty in both cases was estimated using the AES (approximate error scaling) uncertainty estimation method proposed in this work which is based in the idea that the true error is proportional to the approximate error.

In the case of the MS (boundary layer type flow); monotonic convergence was observed only with second order calculations for both velocity components in the vicinity of the wall. Away from the wall first and second order calculations showed monotonic convergence in all the flow variables. The estimated uncertainty performs pretty well in first and second order calculations since it bounds the true uncertainty. It was observed that the uncertainty estimation method performs better when coarse triplets are used. Therefore, it can be said that the methodology presented in here to estimate uncertainty is valid not only in the asymptotic range since coarse grids have been used and the method performs better with coarse grids. Also it has been shown that the proposed method is not restricted to be used for cases converging monotonically.

In the BFS case non-monotonic convergence was observed in most of the points of interest and flow variables when the Spalart-Allmaras and standard k-ε turbulence model were used with first and second order discretization schemes. The estimated uncertainties in the local flow variables and the reattachment point with the Spalart-Allmaras model were smaller than those calculated with the standard k-ε model. In the integral quantities the opposite behavior was observed. Comparison of the numerical results with experimental data shows that the standard k-ε model predicts the flow field better than the Spalart-Allmaras model. In fact, when the validation uncertainty is used along with the numerical results, the results obtained with the standard k-ε model bounds the experimental data better than those obtained with the Spalart-Allmaras model.

In case of 1st order upwind scheme the difference between the two turbulence model predictions is in the order or slightly larger than the discretization error, whereas in case of 2nd order scheme this difference is usually less than or in the same order as the discretization error. In conclusion, the performance of these two models seems to be very similar for the case of BFS application.

APPENDIX: On the Relation of AES method to RE

The AES method assumes that the extrapolated error to zero grid size (here and after referred to as E_t) is proportional to the approximate error defined in an ordered manner as follows

$$E_t = \phi - \phi_{i+1} = C\left(\phi_i - \phi_{i+1}\right);\ \ i = 1,2,3..... \tag{A1}$$

Such that $h(i) = \alpha h(i+1)$ where α<1.0 is the grid refinement factor .Equation (A1) does not make any explicit assumption about E_t being a power series expansion, hence does not require any calculation or use of the apparent order, p. Writing the above equation for i=1 and 2 and solving for C yields

$$C = \frac{\phi_3 - \phi_2}{\phi_3 - 2\phi_2 + \phi_1} \tag{A2}$$

for the local value of the error scaling factor C. The assumption here is that the first and the second differences that appear in the numerator and the de-numerator of Eq. (A2) reflects the

characteristics of the numerical scheme used to produce these numerical solution, hence it is an ordered approximation, but the order need not be known explicitly.

However, if one is to assume that E_t can be expressed in terms of a Taylor series, then relations can be derived for C that will explicitly relate it to the grid size, h, and the refinement factor α. For example let us assume that

$$E_t = b_1 h + b_2 h^2 \tag{A3}$$

Using Eqs. (A1) and (A2) it can be shown that

$$C = \left\{ 1 - \frac{\alpha\left[b_1 + b_2 \alpha h \left(1+\alpha\right) \right]}{b_1 + b_2 h \left(1+\alpha\right)} \right\}^{-1} \tag{A4}$$

Eq (A4) shows that C is indeed an ordered parameter. Moreover, in the asymptotic range it attains values of 2 and 4/3 for a first order method ($b_2 = 0$) and a second order method ($b_1 = 0$), respectively, in the case of grid doubling, i.e. $\alpha = ½$. Similar relations can be derived for other cases depending on how the Taylor series is represented in terms of α and h. But it should be emphasized again that Taylor series expansion of E_t is not required for application of AES method.

REFERENCES

[1] Celik I, Li J. Assessment of numerical uncertainty for the calculations of turbulent flow over a backward facing step. *International Journal for Numerical Methods in Fluids* 2005; **49**:1015–1031.

[2] Proceedings of the *Workshop on CFD Uncertainty Analysis*, held in Lisbon, October, 19th and 20th, 2006 at Instituto Superior Técnico.

[3] David M. Driver, H. Lee Seegmiller, Features of a Reattaching Turbulent Shear Layer in Divergent Channel Flow. *AIAA Journal* 1995; Vol. 23, Nº 2, 163-171.

[4] Eça, L. and Hoekstra, M., On the Influence of the Iterative Error in the Numerical Uncertainty of Ship Viscous Flow Calculations, *26th Symposium on Naval Hydrodynamics*, Rome, Italy, 17-22 September, 2006.

[5] Ferziger, J.H., Estimation and Reduction of Numerical Error, *ASME Winter Annual Meeting*, San Francisco, December, 1989

[6] Ferziger, J.H., Peric, M., Further Discussion of Numerical Errors in CFD, *International Journal for Numerical Methods in Fluids*, 1989; **23**: 1263-1274.

[7] Stern, F., Wilson, R., and Shao, J. (2006) Quantitative V&V of CFD Simulations and Certification of CFD Codes. *Int. Journal of Numer. Meth. Fluids* 2006; **50**: 1335-1355

[8] Richardson, L.F., The Approximate Arithmetical Solution by Finite Differences of Physical Problems Involving Differential Equations, with an Application to the Stresses In a Masonary Dam, *Transactions of the Royal Society of London* 1910; Ser. A, **210**: 307-357.

[9] Richardson L.F. and Gaunt, J. A., The Deferred Approach to the Limit, *Philos. Trans. R. Soc. London* 1927*; Ser. A*, **226**: 299-361.

[10] Celik, I., Chen, C.J., Roache, P.J. and Scheurer, G. Editors., Quantification of Uncertainty in Computational Fluid Dynamics, ASME Publ. No. FED-Vol. 158, *ASME Fluids Engineering Division Summer Meeting*, Washington, DC, 20-24 June, 1993.
[11] Celik, I., Karatekin, O., Numerical Experiments on Application of Richardson Extrapolation With Nonuniform Grids, *ASME Journal of Fluid Engineering* 1997, **119:** 584-590.
[12] Eca, L. and Hoekstra, M., An Evaluation of Verification Procedures for CFD Applications, *24th Symposium on Naval Hydrodynamics*, Fukuoka, Japan, 8-13 July, 2002.
[13] Freitas, C.J., Journal of Fluids Engineering Editorial Policy Statement on the Control of Numerical Accuracy, *Journal of Fluids Engineering* 1993, **115:** 339-340.
[14] Roache, P.J., A Method for Uniform Reporting of Grid Refinement Studies, Proc. of Quantification of Uncertainty in Computational Fluid Dynamics, Edited by Celik, et al., *ASME Fluids Engineering Division Spring Meeting*, Washington D.C., June 230-240, 1993, ASME Publ. No. FED-Vol. 158.
[15] Roache, P. J., Verification and Validation in Computational Science and Engineering, Hermosa Publishers, Albuquerque, 1998.
[16] Stern, F., Wilson, R. V., Coleman, H. W., and Paterson, E. G., Comprehensive Approach to Verification and Validation of CFD Simulations - Part 1: Methodology and Procedures, *ASME Journal of Fluids Engineering* 2001; **123:** 793-802.
[17] Broadhead, B.L., Rearden, B.T., Hopper, C.M., Wagschal J.J., Parks,C.V., (2004), Sensitivity- and Uncertainty-Based Criticality Safety Validation Techniques, *Nuclear Science and Engineering* 2004, **146:** 340–366.
[18] DeVolder, B., Glimm, J., Grove, J. W., Kang, Y., Lee, Y., Pao, K., Sharp, D. H., Ye, K., Uncertainty Quantification for Multiscale Simulations, *Journal of Fluids Engineering* 2002, **124**, Issue 1: 29-41.
[19] Oberkampf, W.L., Trucano, T.G., and Hirsch , C., Verification, validation, and predictive capability in computational engineering and physics, Sandia Report SAND2003-3769.
[20] Elizalde-Blancas F., Celik I. B., Verification of Various Measures for Numerical Uncertainty Using Manufactured Solutions, Proceedings of the 2nd Workshop on CFD Uncertainty Analysis, October 19-20, 2006, Lisbon, Portugal.
[21] Celik I, Li J, Hu G, Shaffer C., Limitations of Richardson extrapolation and some possible remedies. *ASME Journal of Fluids Engineering* 2005; **127**:795 –805.
[22] Celik I, Karaismail E., Parsons D., A Reliable Error Estimation Technique for CFD Applications, AVT-147 Symposium on Computational Uncertainty in Military Vehicle Design, December 3-6, 2007 Athens, Greece.